Laser and Particle Beams (2003), *21*, 85–89. Printed in the USA.

DOI: 10.1017/S0263034603211162

Phase space growth during RF capture in the GSI heavy ion synchrotron SIS-18

M. KIRK, H. DAMERAU, I. HOFMANN, O. BOINE-FRANKENHEIM, P. SPILLER, AND P. HÜLSMANN

Gesellschaft für Schwerionenforschung, Darmstadt, Germany

(RECEIVED 24 June 2002; ACCEPTED 5 November 2002)

Abstract

This study reports on the optimization of the radio frequency capture phase during the operational cycle of the SIS-18 synchrotron at Gesellschaft für Schwerionenforschung, Darmstadt, Germany. The ion species studied were $^{238}U^{+28}$ and $^{238}U^{73+}$ at an injection energy of 11.4 MeV/u. The longitudinal relative momentum spread derived from Schottky spectra of the coasting beam at injection provides a value of $|\Delta p/p_0|_{\text{full-width}} \sim 5 \times 10^{-3}$. Simulation results from the synchrotron tracking code ESME (FermiLab) were compared with beam-current profile measurements obtained from a pickup. To gain further insight, the Tomography program (European Organization for Nuclear Research) has been used to derive the longitudinal phase space development from waterfall plots of the measured beam current profile, which may then be compared against simulation. Possible causes of this nonadiabaticity are discussed and solutions are proposed.

Keywords: Adiabatic capture; Emittance; RF bucket; Tomography; Waterfall plot

1. INTRODUCTION

A radio frequency (RF) gymnastic is called "adiabatic" when the parameters of the synchrotron motion are changed slowly enough for the distribution of particles to be at equilibrium along the whole process (Lilliequist & Symon, 1959). The RF capture of a DC coasting beam in a synchrotron just after injection should, in principle, be adiabatic. In reality, this is known not to be the case. One observes what is perceived to be a rapid bunch formation within ~2 ms, which is much shorter than the rise time of the cavity voltage (typically ~40 ms). An adiabatic capture process should keep any beam losses to a minimum. Furthermore, such a process, through its ability to preserve the beam's emittance, enables a more efficient bunch "rotation" scheme in phase space whereby the final bunch length at the target is minimized. This makes possible not only the study of plasmas at higher energy densities, but would also be of potential benefit to the design of the Heavy Ion Driven Ignition Facility (HIDIF) which would be used to ignite D-T fuel pellets (Hofmann, 2000).

The heavy ion synchrotron SIS-12/18 at Gesellschaft für Schwerionenforschung (GSI) shall become a booster for the future SIS-100/200, which should deliver higher intensity beams, as high as 2.5×10^{11} for $^{238}U^{28+}$ and 4×10^{10} for $^{238}U^{73+}$, accelerated to higher energies. Emittance growths during RF capture have been determined from beam position monitor (BPM) measurements in the GSI synchrotron SIS-18 to be ~100% (Liu *et al.*, 2000). This work reports on the cause of this emittance growth and solutions are proposed.

Address correspondence and reprint requests to: M. Kirk, GSI mbH, Planckstr. 1, d-64291 Darmstadt, Germany. E-mail: m.kirk@gsi.de

2. MODELING

The ESME version 2001 particle-in-cell (PIC) simulation code (MacLachlan, 1988) was used to calculate the longitudinal phase space distribution of the beam. The energy and phase of the ith particle relative to the synchronous particle (the sth particle) were tracked at regular intervals along the ring, in this case every turn. The tracking equations were

$$\begin{aligned} \vartheta_{i,n} &= \left[\frac{\tau_{s,n-1}}{\tau_{s,n}} \vartheta_{i,n-1} + 2\pi \left(\frac{\tau_{i,n}}{\tau_{s,n}} - 1 \right) \right]_{\text{mod}(\pi)} \\ E_{i,n} &= E_{i,n-1} + eV(\varphi_{s,n} + h\vartheta_{i,n}) - eV(\varphi_{s,n}), \end{aligned} \tag{1}$$

where τ is the revolution period. The beam was represented as 10^5 macroparticles. The noise growth in the code was determined for a DC coasting beam scenario (mean energy 11.4 MeV/u, $\delta P/P_0(FWHM) = 5 \times 10^{-4}$, and 10^5 macroparticles). It was found that the rms longitudinal spread in

energy of the beam increased by 1% after 16,000 machine turns; on the time scale of the capture process. The impedance from cavities may be represented by the equivalent circuit representation of a LRC resonant circuit:

$$Z_{\parallel}^{cav} = \frac{R_{shunt}}{1 + iQ(\omega/\omega r - \omega r/\omega)}. \quad (2)$$

The impedance from the space charge of the beam is described by

$$\frac{Z_{\parallel}^{sc}}{n} = -\frac{igZ_0}{2\beta\gamma^2} \quad (3)$$

where

$$g = \frac{g_0}{1 + n^2/n_c^2}\,(n_c \approx R/b).$$

Resistive wall impedances had to be implemented through look-up tables. This type of impedance is given by

$$\frac{Z_{\parallel}^{res}}{n} = (1 + i)\frac{R}{\sigma_w \delta_{s0}}\frac{1}{\sqrt{n}} \quad (4)$$

where δ_{s0} is the skin depth at beam harmonic $n = 1$. The input data for the voltage and magnetic field ramps used to drive the synchrotron were produced by the ZYKLOP program (Franczak, 2000). The fixed parameters during the studies of the SIS were specified in ESME as given in Table 1.

3. RESULTS AND DISCUSSION

The initial frequency of the DC beam was measured with a Fourier Spectrum Analyzer with a 1-GHz bandwidth. The dwell time of the beam in SIS was 200 ms, which allowed enough time for the microbunch structure (at 36 MHz) from the LINLAC to dissipate therefore leaving just the Schottky noise of the DC beam to detect. A typical spectrum from an uncooled beam is shown in Figure 1. Such a large relative momentum spread is normally undesirable, here 4.2×10^{-3} full width (6σ), determined from

$$\frac{\Delta P}{P} = \left|\frac{1}{\eta}\frac{\Delta f}{f}\right| \quad (5)$$

where the slip factor $\eta = \alpha - \gamma^{-2}$. This large longitudinal momentum spread is believed to come from errors in the synchronism between the voltage signals fed to the drift tube elements of the Alvarez type LINAC, which result in fluctuations in the mean energy from bunch to bunch. It may also be noticed that the center frequency of the distribution in Figure 1 is not exactly an integer number of the known revolution frequency (~213 kHz). Thus we have an energy discrepancy in this case of about 0.0059 MeV/u above the synchronous kinetic energy of 11.145 MeV/u.

The effect of this energy mismatch on the beam in phase space has been simulated with the use of ESME and is shown in Figure 2. We can see that the effect is to increase the final emittance at 58 ms, after the RF voltage is turned on, by ~70%. It is also of interest to note that the beam is left in a state of persistent dipole motion, that is, there is no Laudau damping in the presence of strong space charge (O. Boine-Frankenheim & Y. Liu, pers. comm.).

The same effect may be confirmed qualitatively from the phase space derived from a pickup measurement of the line-charge density profile over several turns spanning approximately one synchrotron period. The CERN Tomography code (Hancock *et al.*, 2000) was used for this purpose. The pickup reading for a carbon beam is shown in Figure 3. At the onset of bunching there are two stong peaks in the envelope of the signal. These are due to the presence of two bunch barycenters in the bucket, such as illustrated in the top right panel of Figure 2.

Before the Tomogaphy code was used to determine the phase space distribution from experimental data, a benchmark test was performed. A simple bunch rotation scenario under significant space-charge conditions was produced in ESME. The waterfall plot generated by ESME was then fed

Table 1. *Description of beam and environment implemented in the ESME computer model*

Smooth wall toroid	
Major radius (R), minor radius (b)	34.492 m, 0.05 m
Initial phase space distribution of the DC coasting beam at injection	Random uniform in azimuth ($-\pi$ to π rad) and parabolic in energy about the synchronous energy
Transverse phase space of the beam assumed at injection	Uniform circular. Radius 0.03 m
Impedance from RF accelerating cavity	Shunt impedance $R_{\text{shunt}} = 3\text{k}\Omega$, quality factor $Q = 10$, resonant frequency ω_r matched to h = 4th harmonic of beam revolution frequency at injection.
Other impedances included	Direct space charge, resistive stainless steel wall impedance.
Broad band impedance	Negligible.
Number of macroparticles	10^5
Transition gamma γ_T ($\alpha = \gamma_T^{-2}$)	5.45

https://doi.org/10.1017/S0263034603211162 Published online by Cambridge University Press

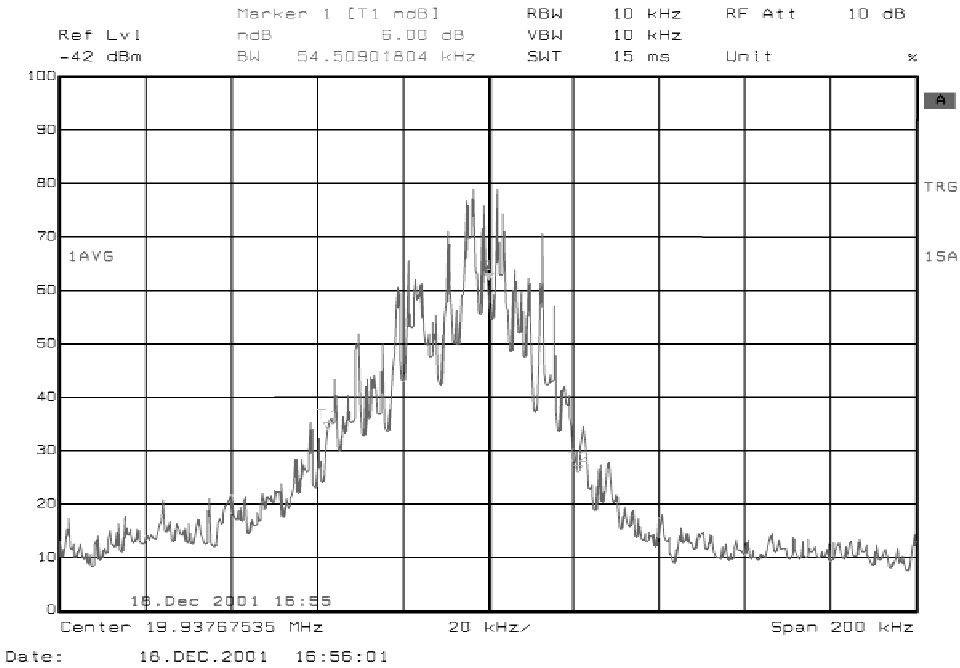

Fig. 1. Schottky spectrum of an uncooled U^{73+} coasting DC beam.

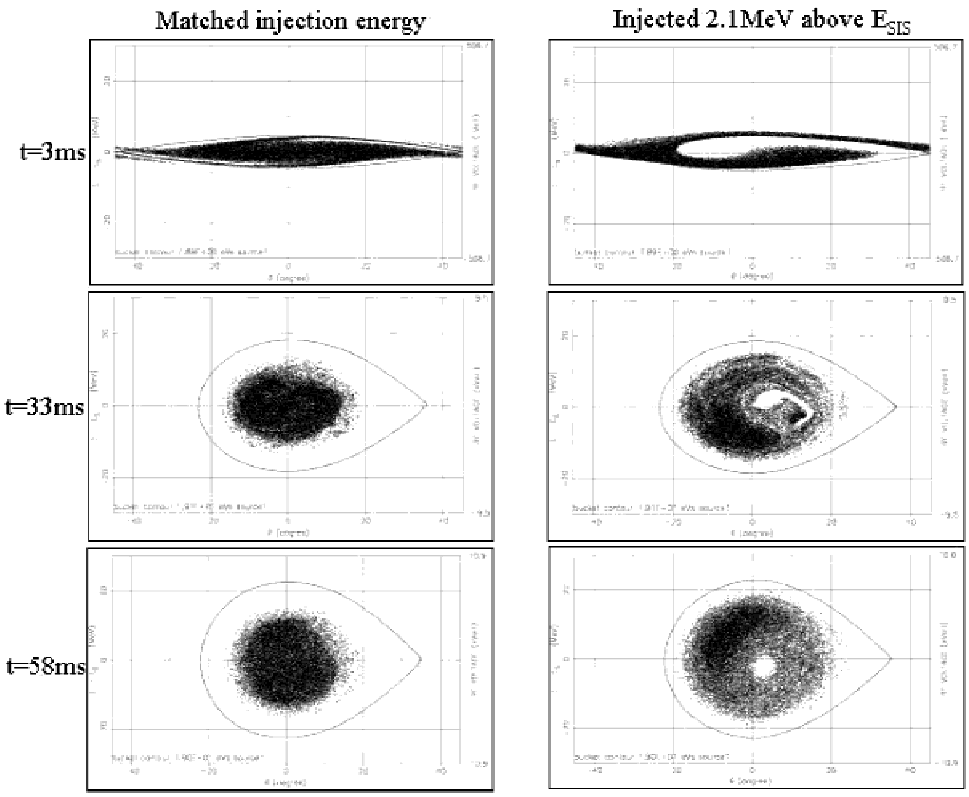

Fig. 2. ESME simulation of phase space during capture. The initial energy spread of the DC beam was taken as the typical quoted FWHM value of $\delta P/P = 5 \times 10^{-4}$, or $\delta E_{FWHM} = 5.236$ MeV. Since a parabolic energy profile was assumed in the simulation this energy spread was considered to be equal to the cut-off limits of the energy distribution. *X*-axes run from $-45°$ to $45°$. *Y*-axes run from -30 MeV to 30 MeV.

https://doi.org/10.1017/S0263034603211162 Published online by Cambridge University Press

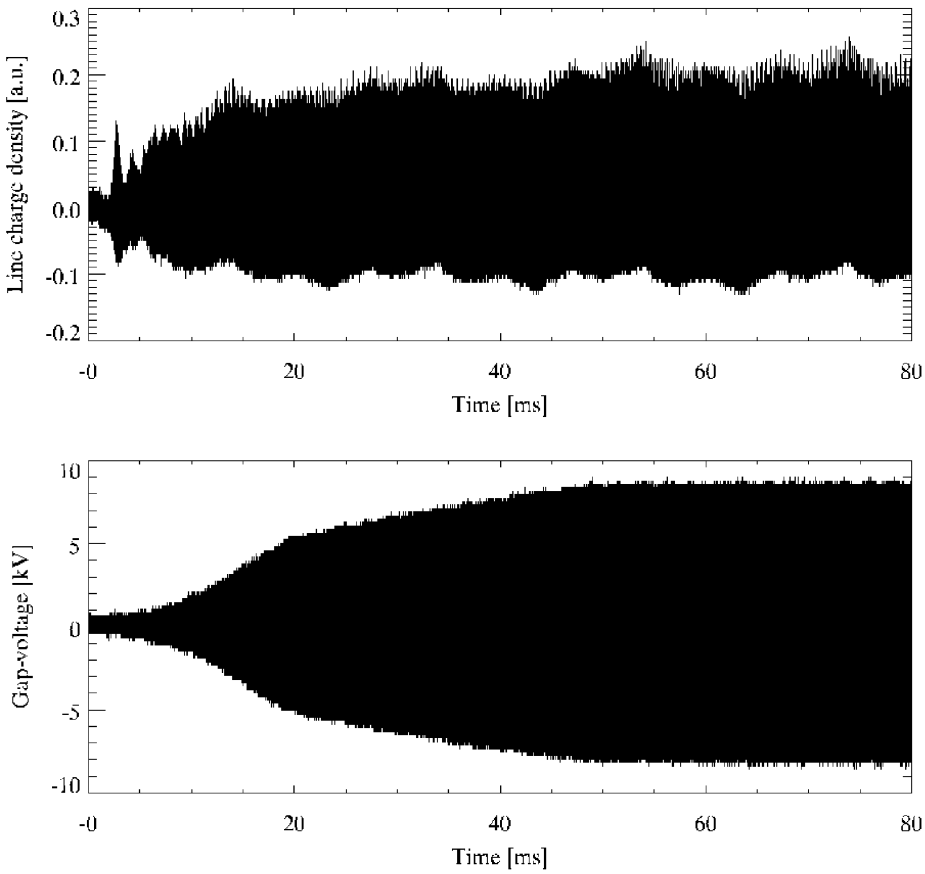

Fig. 3. Line charge density profile of $^{12}C^{6+}$.

into the Tomography algorithm. The original phase space was accurately reconstructed by the Tomography algorithm. The algorithm was even capable of resolving the fine phase space dilution resulting from the nonlinearity in the phase space motion in the bucket. Finally, Figure 4 shows the phase space derived from the $^{12}C^{6+}$ RF capture experiment. There is a clear halo present in the distribution which tallies with the halo distribution in Figure 2, bottom right panel.

4. CONCLUSIONS

It has been found that the energy discrepancy between the Linac and the synchronous energy of SIS is the major cause of emittance growth in SIS. The beam losses during RF capture, which were measured with a DC transformer, are ~30%. Most of this loss is caused by the exceptionally large momentum spread of the uncooled beam, which is larger than the momentum acceptance of SIS at the end of the capture process, and furthermore that those particles outside the separatrix of the RF bucket, during acceleration, are lost to the walls. Energy offset at injection may also give rise to emittance increase in the transverse (horizontal and vertical) planes due to the presence of dispersion.

High intensity beams, in which space charge is significant, may have to be damped through fast-acting feedback systems to avoid dipole motion forming, if a precise and well-matched energy from the Linac cannot be realized. Iso-adiabatic voltage ramp forms have recently been tested in machine experiments (not reported here); first observa-

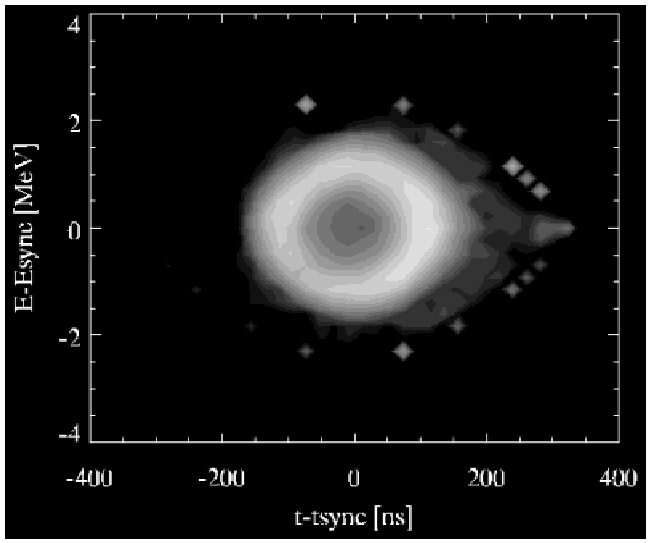

Fig. 4. Phase space from experimental pickup measurements of a $^{12}C^{6+}$ beam.

https://doi.org/10.1017/S0263034603211162 Published online by Cambridge University Press

tions from Schottky spectrum measurements of the DC beam, before and after the bunch-accelerate-debunch process, suggest that the emittance growth is significantly lower than the presently commissioned ramps, for the same period of time.

REFERENCES

FRANCZAK, B. (2000). Program ZYKLOP, Version 833. Darmstadt, Germany: GSI.

HANCOCK, S., LINDROOS, M. & KOSCIELNIAK, S. (2000). Phys. Rev. Special Topics—Accelerators and Beams, **3**, 124202-4–124202-6.

HOFMANN, I. (2000). Heavy Ion Inertial Fusion in Europe. Proc. Conf. San Diego.

LILLIEQUIST, C.G. & SYMON, K.R. (1959). Deviations from adiabatic behaviour during capture of particles into an R. F. Bucket. MURA Internal Report. MURA-491. Madison, Wisconsin.

LIU, Y., SPILLER, P. & HOFMANN, I. (2000). A measurement of momentum spread variation in SIS capture-acceleration-debunching process. GSI report. Darmstadt, Germany: GSI.

MACLACHLAN, J. (1990). Fundamentals of particle tracking for longitudinal projection of beam phase space in Synchrotrons, FermiLab note, FN-481 (15 April, 1990), Batavia, Illinois.

https://doi.org/10.1017/S0263034603211162 Published online by Cambridge University Press